

# Capillary filling speed in silicon dioxide nanochannels

S.E. Jarlgaard, M.B.L. Mikkelsen, P. Skaftø-Pedersen, H. Bruus, and A. Kristensen

MIC - Department of Micro and Nanotechnology, NanoDTU, Technical University of Denmark  
Bldg. 345 east, DK-2800 Kongens Lyngby, Denmark, ak@mic.dtu.dk

## ABSTRACT

We present a simple silicon-based fabrication technique for nanocapillaries based on controlled growth of silicon-dioxide, UV lithography, etching with etch-stop, and glass wafer bonding. Our approach improves state-of-the-art with respect to the obtained cross-wafer homogeneity and precision in the height of the nanocapillaries. The improvement is due to our use of the silicon substrate as an etch stop. We extend the results in Tas *et al.*, Appl. Phys. Lett. **85**, 3274 (2004), by measuring capillary filling speed on seven different channel heights, ranging from 25 to 3400 nm. A systematic deviation from bulk behaviour has been observed for channel heights below 100 nm.

**Keywords:** nanofluidics, nanochannels, capillary filling, nanofabrication

## 1 Introduction

Our work is motivated by recent experiments involving stretching of individual DNA molecules in nanochannels [1]. Simple, reproducible fabrication of nanochannels, and understanding the basic nanofluidics is instrumental for further advancement of this technology. In addition to the deposition-based fabrication approach in Ref. [1], two other methods have been reported recently: TMAH etched silicon plus a single oxidation step without etch stop resulting in accuracies of  $h = \pm 3$  nm [2], and similar results obtained by using reactive  $\text{CHF}_3/\text{O}_2$  plasma etch into fused silica [3] or commercial buffered oxide etchant for etching into Borosilicate glass [4].

## 2 Fabrication of nanochannels

In Fig. 1(a)-(d) we outline our four main process steps, where nanometer homogeneity and precision in the final channel height  $h$  is obtained by means of thermal oxidation and wet etching: (a) On a silicon wafer substrate we grow a primary thermal oxide layer of thickness  $h + d$ . (b) The nanofluidic channel is defined by UV lithography and wet-etching in buffered hydrogen fluoride (BHF) that removes exposed silicon-dioxide all the way down to the silicon substrate. This leaves channels with silicon-dioxide side-walls of height  $h + d$  and

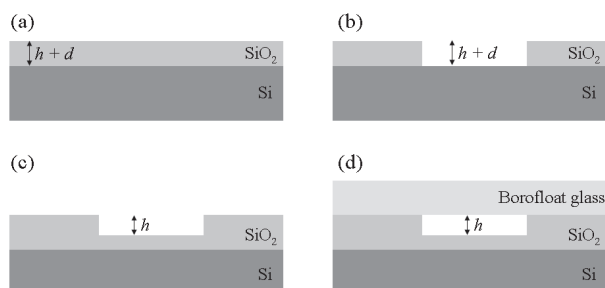


Figure 1: Outline of the four main process steps, where nanometer precision in the final channel height  $h$  is obtained by means of thermal oxidation and BHF wet etching, see text.

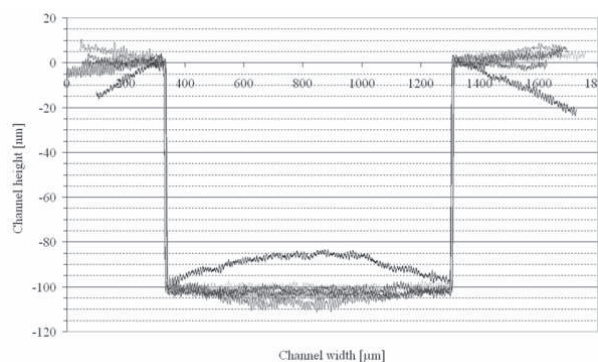


Figure 2: Superposed surface profiler scans across 100 nm channels at various places on a 100 mm wafer. The step height is seen to be very uniform and thus the process is well suited for making nanochannels with a very low tolerance of  $\pm 2$  nm. A small amount of stress appears, but it does not affect the step height.

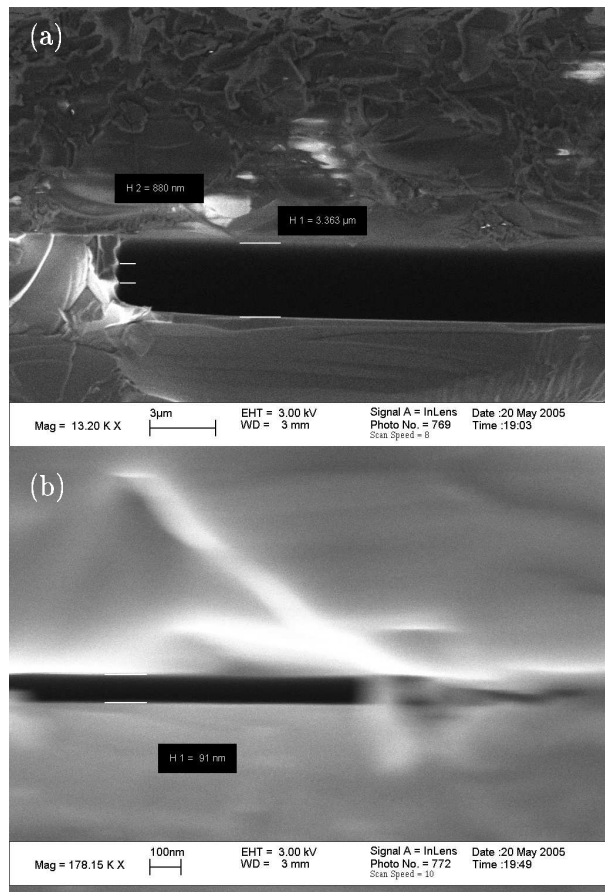


Figure 3: SEM pictures of channel cross-sections of cleaved devices. (a)  $3.4 \text{ }\mu\text{m}$  channel showing  $h = 3363 \text{ nm}$ . (b)  $100 \text{ nm}$  channel showing  $h = 91 \text{ nm}$ .

a silicon floor. (c) A second oxidation step is applied to obtain a silicon-dioxide floor. The growth rate of silicon-dioxide decreases with increasing oxide thickness. Consequently, the secondary oxidation is faster inside the channel region than in surroundings, and the channel height decreases as the growth progresses. The secondary oxidation is stopped when the channel height is reduced from  $h + d$  to desired value  $h$ . The oxidation times, which determine the heights  $h + d$  and  $h$ , were found from computer simulations using the software *SUPREM*. (d) A borofloat glass lid is bonded to the make a sealed, hydrophilic, all-silicon-dioxide channel. Channels,  $15 \text{ mm}$  long, of heights  $h$  from  $25 \text{ nm}$  to  $3 \text{ }\mu\text{m}$ , widths from  $20 \text{ }\mu\text{m}$  to  $500 \text{ }\mu\text{m}$  were realized. The channels tend to collapse for the largest width to height ratios.  $25 \text{ nm}$  high channels were realized with channel widths up to  $50 \text{ }\mu\text{m}$ , similar to results reported recently by Mao and Han [4].

By use of a surface profiler we have found that our "oxidation, etch-stop, oxidation" sequence leads to an

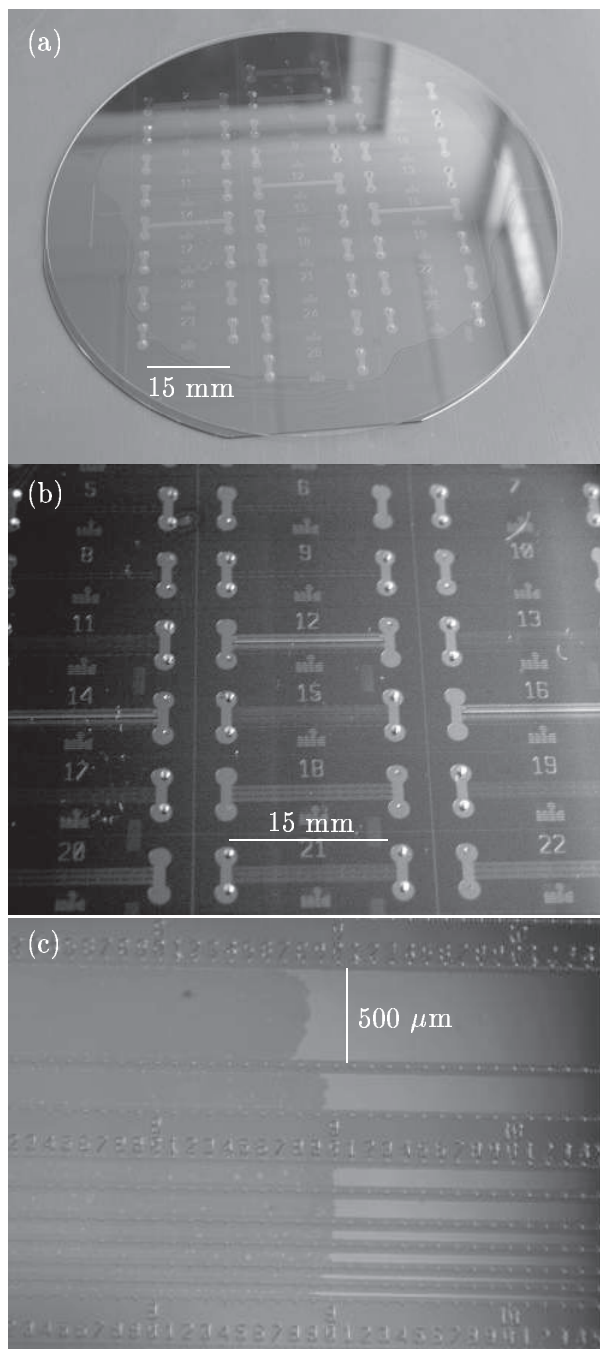


Figure 4: Nanofluidic channel devices, fabricated on  $100 \text{ mm}$  silicon wafer substrates. (a) The  $100 \text{ mm}$  wafer, containing 26 chips, each with 9 parallel nanochannels. (b) Zoom in on individual chips, showing the nanochannels connecting inlet and outlet reservoirs. (c) A microscope picture of the liquid fronts, shown as the dark areas, in a chip with  $100 \text{ nm}$  high channels. The smallest marks on the chip are placed  $25 \text{ }\mu\text{m}$  apart.

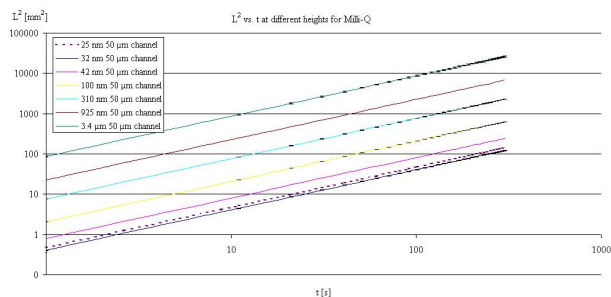


Figure 5: Measured capillary filling speed for milli-Q water in nanochannels shown as a log-log plot of the square  $L^2$  of the front-meniscus position  $L$  versus time for seven different channel heights  $h$  ranging from 25 to 3400 nm. All curves have the expected linear form  $L^2 = at$ .

improved precision of  $\pm 2$  nm in the channel height  $h$ , see Fig. 2.

The profile of the sealed nanochannels was assessed by SEM inspection of cleaved samples. In Fig. 3 we show cross-sectional images of 3.4  $\mu\text{m}$  and 100 nm high nanochannels.

### 3 Capillary filling speed

Our measurements by optical microscope and video camera of capillary filling speeds include seven 50  $\mu\text{m}$  wide channels with heights ranging from 25 to 3400 nm, thus extending previously reported height ranges, [2], [3]. The position of the front meniscus during capillary filling is denoted  $L(t)$ . As expected from the combined effect of capillary pressure and hydraulic resistance [2],

the square of the position increases linearly in time,  $L^2(t) = at$ , see Fig. 5. However, as seen in Fig. 6, for channel heights  $h$  below 100 nm the measured slopes  $a$  are systematically larger than the expected slope  $a_{\text{bulk}}$ . The origin of this effect is currently under study.

## 4 Conclusion

In conclusion, a simple and well-controlled fabrication technique has been achieved, and in subsequent measurements of capillary filling, we have identified a threshold height of about 100 nm, below which deviations from bulk fluidics are significant.

## Acknowledgements

The partial support of the EC-funded project NaPa (Contract no. NMP4-CT-2003-500120) is gratefully acknowledged. The content of this work is the sole responsibility of the authors.

## REFERENCES

- [1] W. Reisner, K. J. Morton, R. Riehn, Y. M. Wang, Z. Yu, M. Rosen, J. C. Sturm, S. Y. Chou, E. Frey, and R. H. Austin, Phys. Rev. Lett, **94**, 196101, 2005.
- [2] N.R. Tas, J. Hanevel, H. Jansen, M. Elwenspoek, A. van den Berg, Appl. Phys. Lett. **85**, 3274, 2004.
- [3] F.H.J. van der Heyden, D. Stein, and C. Dekker, Phys. Rev. Lett. **95**, 116104, 2005.
- [4] P. Mao and J. Han, Lab Chip **5**, 837, 2006.

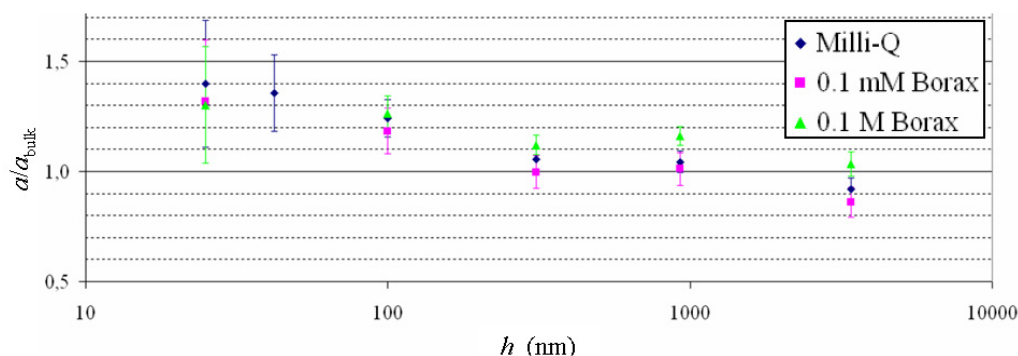


Figure 6: Slopes  $a$  (see Fig. 5) for three different liquids (normalized by the theoretical bulk value  $a_{\text{bulk}}$  obtained from contact angle measurements) as a function of channel height  $h$ . A systematic increase is observed for decreasing  $h$  below 100 nm.